



ELSEVIER

Computer Physics Communications 108 (1998) 20–28

Computer Physics  
Communications

# Finding tracks detected by a drift tube system

S. Baginyan, G. Ososkov<sup>1,2</sup>

*Joint Institute for Nuclear Research, Laboratory of Computing Techniques and Automation, Dubna, 141980, Russian Federation*

Received 24 August 1997; revised 30 October 1997

## Abstract

An algorithm for track recognition, based on a combination of the robust track fit and the deformable template method, is proposed for data detected by a system of drift tubes. Dependencies of the algorithm efficiency and the radius of recognized tracks on the measurement errors are explored with simulated events. © 1998 Elsevier Science B.V.

## 1. Introduction

A conventional track recognition problem can be considered as an exhaustive sorting of all data points recorded by a track chamber into a “sufficient” number of subsets (track candidates). Each subset must satisfy conditions of “sufficient” smoothness of alignment along a straight line or a higher-order curve corresponding to the absence or presence of the magnetic field. The notion “sufficient” depends on statistical efficiency requirements of the given experiment to both the track reconstruction methods and the statistical criteria applied.

For instance, the smoothness of the data point alignment for a track candidate can be fulfilled by fitting a second order curve to each of 2D projections of these points applying then the  $\chi^2$ -criterion. The efficiency of the track reconstruction algorithm depends, basically, on the “reasonability” of the clustering method applied to group data points into track candidates. It determines both the highest probability of the real track to be found and the lowest chance to include a “ghost”

track to track-candidates. Besides, such a reasonability has to guarantee the maximum possible reduction of the search trials made by the used method over all points in order to minimize the computer time consumption. As examples of such reasonable algorithms, one can point out well-known methods like variable slope histogramming or track following (stringing) methods [1–3], as well as relatively new approaches like Hopfield neural networks [4,5].

Drift tubes are one of the detector systems widely used in modern high energy physics experiments ([6–8]). Below we use the ATLAS Monitored Drift Tube (MDT) setup [6] as an example. Each time when a passing particle track hits a tube, it registers two data: its own center coordinates and the drift radius, i.e. the drift distance between the particle tracks and the anode wire placed in the center of this tube. Thus, a track passing the MDT provides a set of anode wire coordinates and corresponding drift radii. Unfortunately, some of these data can be lost due to the tube inefficiency. In addition, a number of noise coordinates is also recorded. However, the main problem which hinders applications of the above-mentioned conventional track recognition methods, is the left–right ambiguity of drift radii. There is no information on which side of

<sup>1</sup> Supported by RFFI, grant N 97-01-01027, Russian Federation.

<sup>2</sup> E-mail: osg@lcta39.jinr.dubna.su

the anode wire the track passed. The anode wire coordinates themselves are very rough indicators of particle locations. So if one would even recognize a subset of these tubes belonging to a concrete track and would then approximate it by a second-order curve (circle or parabola), the resulting parameter accuracy would not be satisfactory.

In this report, a combined algorithm for track recognition in a uniform magnetic field is proposed for the muon spectrometer drift tube design corresponding to the MDT system of the ATLAS experiment. As it follows from the ATLAS proposals [6], the ATLAS muon spectrometer is divided into 8 sectors (called ROI – Regions of Interest). Those sectors are designed in such a way that despite the extremely high multiplicity of ATLAS events, the mean number of muon tracks in each ROI should not exceed 1–2 per event (see the table on page 140 of [6]). This important consideration conditioned our choice of methods to be sufficiently accurate and efficient for off-line MDT data processing.

The problem formulation is reduced to the  $(x, y)$  plane perpendicular to the magnetic field and anodes of drift tubes where track projections can be considered as arcs of a circle. Our algorithm combines effectively a robust track fit [9] and our modification of the deformable template method [10,11]. Both methods need initial conditions for templates. The ATLAS design is supposed to be able to provide such initial conditions from the RPC (Resistive Plate Chambers [6]) trigger system. However, we had no information yet about RPC data, so for more generality we used a Hough transform modification to obtain the number of circle arc templates and rough estimations of their parameters on the very first stage of MDT data processing.

The paper is organized as follows: in Section 2 we formulate the problem. The next section describes a modified Hough transform. Sections 4 and 5 contain brief descriptions of the robust fitting and deformable template algorithms. Details of the hybrid algorithm are given in Section 6. Results on simulated data are presented in Section 7. Finally, in Section 8 the reader finds our conclusions.

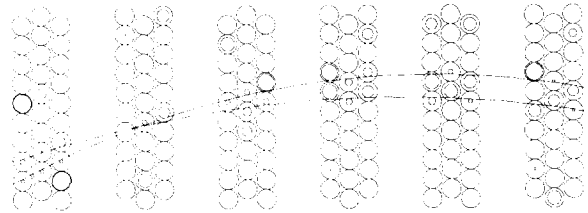


Fig. 1. Example of a typical event.

## 2. Formulation of the problem

The MDT system for one of the ROI of the ATLAS muon spectrometer consists of the modules formed by several layers of tubes arranged in honeycomb order (see Fig. 1). In the middle of every tube there is an anode wire with known  $XY$ -coordinates. All tracks of an event passing these layers produce  $N$  signals, i.e. set  $M = \{x_i, y_i; r_i, i = \overline{1, N}\}$ , where  $(x_i, y_i)$  are coordinates of the hit tube centers,  $r_i$  are drift radii. Let us suppose, first, that the recognition problem is solved, i.e. the subset  $S$  of triplets  $(x_i, y_i; r_i)$  produced by only one of the tracks and, probably, also by some noise level tubes was extracted from the set  $M$ . For the sake of simplicity, let us keep for  $S$  the same notation as for  $M$ , i.e.  $S = \{x_i, y_i; r_i, i = \overline{1, N}\}$ . Geometrically the set  $S$  can be considered as a set of circles on the plain with centers  $(x_i, y_i)$  and radii  $r_i$ .

Thus, *the mathematical formulation of the problem* is to draw the track line as a second-order curve (circle or parabola) tangential to the maximum number of these small circles (SC) from  $S$ .

To clarify our approach, we introduce a new concept of *the measure of tangency* of an arbitrary curve  $y = f(x)$  to one of SCs  $(x_i, y_i; r_i)$  as the difference  $D_i(f)$  between two values: the SC radius  $r_i$  and the distance from its center to the curve  $y = f(x)$ . In the obvious case, when a curve and SC are tangential, their tangency measure is equal to zero:  $D_i(f) = 0$ . Thus using the measure of tangency concept for an arbitrary track model  $y = f(x)$ , we reduce our problem to minimizing the functional

$$L = \sum_{i=1}^N D_i^2(f). \quad (1)$$

For instance, considering a parabola  $y = Ax^2 + Bx + C$  as the track model, we should find the parabola  $(A, B, C)$  that minimizes the sum of squares of its

tangency measures  $D_i(A, B, C)$  for all SCs from the set  $S$ .

The straightforward determination of a parabola's tangency measure as

$$D_i(A, B, C) = \min_{\{x,y\}} \{ \sqrt{(x_i - x)^2 + (y_i - y)^2} \}, \quad (2)$$

where  $(x, y) \in Ax^2 + Bx + C$ , leads to a nonlinear problem. However, it can be avoided by a linearization of (2). Replacing the parabola by its tangent in the vicinity of  $(x_i, y_i; r_i)$ , one obtains

$$D_i(A, B, C) \approx \frac{A(x_i^2 + R_{\text{tub}}^2/4) + Bx_i + C - y_i}{\sqrt{(2Ax_i + B)^2 + 1}},$$

where  $R_{\text{tub}}$  is the drift tube radius.

The situation looks easier when the track model is a circle  $(a, b, R)$ . The *measure of tangency of two circles* in a plane is the minimum distance between crossing points of these circles with the straight line linking their centers. It is obvious again, when two circles are tangent, their tangency measure is equal to zero.

Now we can take into account the left–right ambiguity problem. Since the variable

$$D_i(a, b; R) = \sqrt{(x_i - a)^2 + (y_i - b)^2} - R \quad (3)$$

can have both positive and negative values, summands in (1) must be twofold,

$$\begin{cases} d_i^- = (D_i(a, b; R) - r_i)^2, & \text{if } D_i(a, b; R) > 0, \\ d_i^+ = (D_i(a, b; R) + r_i)^2, & \text{otherwise.} \end{cases} \quad (4)$$

Thus our problem in the case of the circular track model reduces to minimizing (1) with such dual summands.

In the known literature about circle fitting [12–15], we distinguish two most promising approaches:

- Robust fit derived from the maximum likelihood method [15] (see also programming details in [16])
- Elastic Arm approach similar to [17,18].

Our idea is to combine both methods in one *hybrid algorithm* in order to achieve the maximum efficiency and speed of the drift tube track recognition. In this hybrid algorithm the robust method, as the faster one, is used first, unless its results are satisfactory

( $\chi^2$  goodness-of-fit criterium is less than a prescribed cutoff). Otherwise parameters obtained by the robust method are used as initial values for elastic arm algorithm, which is more precise, on the final stage.

To ensure a fast convergence towards a high quality solution avoiding the local minima of (1), either robust or elastic arm algorithms must be initialized with approximate values for the positions of the centers and the radii of the circles. Due to reasons pointed out above at the end of the introduction, we modify the Hough transform method [19] which, following [20], we call the method of sequential histogramming by parameters (SHPM).

### 3. Sequential histogramming method

Let us first suppose  $\Omega = \{X_i, Y_i, i = \overline{1, N}\}$  to be a set of coordinates  $X_i, Y_i$  measured in the process of recording an event with several tracks. So their point coordinates as well as the noise coordinates belong to  $\Omega$ . A circle arc is supposed to be a good approximation for any track.

Let us consider all triplets of points of the  $\Omega$  set. If these three points do not belong to a straight line, one can draw a circle through them. Thus a set of such circle parameters is obtained:  $W = \{a_j, b_j, R_j, j = \overline{1, C_N^3}\}$ . One could imagine a 3D histogram constructed on that  $W$  set as a hilly surface, where hills should most likely correspond to tracks. This idea together with so-called sequential histogramming approach [20] gives us the following algorithm for finding the initial track parameters:

- (1) Circles are drawn through all admissible point triplets. Then the first parameter  $a_j$  of each circle is histogrammed.
- (2) The value  $a_m$  is obtained that corresponds to the maximum of this histogram.
- (3) With  $a_m$  fixed, circles are drawn through all admissible pairs of points from  $\Omega$ . Then the second coordinate  $b_j$  of each circle is histogrammed.
- (4) The value  $b_m$  is obtained corresponding to the maximum of this second histogram.
- (5) With the coordinates of the center  $(a_m, b_m)$  fixed, all admissible circles of radii  $R_j$  are drawn through points of the set  $\Omega$ . Then the  $R_j$  are histogrammed.

(6) The value  $R_m$  is obtained corresponding to the maximum of this third histogram.

The admissibility in steps (1), (3), (5) above means testing the corresponding values by easy cutoff criteria (for instance, each  $R_j$  is tested whether it is inside a prescribed minimal and maximal radius:  $R_{\min}, R_{\max}$ ).

Then the obtained parameters ( $a_m, b_m; R_m$ ) are subjected to more sophisticated tests. If the results are positive, i.e. parameters ( $a_m, b_m; R_m$ ) are accepted as likely track parameters, all measurements corresponding to it are eliminated from the set  $\Omega$  and the whole procedure is repeated starting from step (1).

If the circle ( $a_m, b_m; R_m$ ) is rejected by testing, then the maximum  $R_m$  of the third  $R_j$ -histogram is eliminated and the procedure is repeated starting from step (6). If there are no more peaks in the  $R_j$ -histogram, then the peak  $b_m$  of the second histogram is eliminated and the procedure is repeated starting from step (4) and so on, unless the procedure would find a true circle or all peaks in the second histogram would be eliminated. In this case the peak  $a_m$  of the first histogram is eliminated and the procedure is repeated starting from step (2).

Thus, the method of sequential histogramming by parameters (SHPM) provides a way to “capture” the area where tracks are likely to be situated and provides us with initial parameters of those tracks. In order to apply SHPM, the results of measurements should belong to the  $\Omega$  set, i.e., a set of track point coordinates. However, we deal with the set  $M$  of small circles (SC)  $\{x_i, y_i; r_i, i = \overline{1, N}\}$ , so we have to determine on each of these SCs a point associated with some of the tracks. Supposing that the vertex area from which all tracks of the given event emanate is known, one can roughly determine such a point as a tangent point of the tangent line drawn to each SC  $(x_i, y_i; r_i)$  from the center of the vertex area. However, there are two tangents to each SC and, therefore, we have two possible track points, i.e. left-and-right (or top-and-down) uncertainty. It would not restrain us in applying the SHPM, but it should be kept in mind that the left-and-right uncertainty factor doubles the element number of the set  $\Omega = \{X_i, Y_i, i = \overline{1, 2N}\}$  comparing with the number of elements in the set  $M = \{x_i, y_i; r_i, i = \overline{1, N}\}$  of the conventional SHPM (see, for example [11]). If the vertex area is unknown, we take two possible track points, such as  $(x_i, y_i + r_i), (x_i, y_i - r_i)$ . To decrease the histogramming search domain of the  $\Omega$  set, it is

necessary to use the maximum of a priori information on the tracks in the event.

The SHPM-description given above stresses the importance of the method used to extract a histogram peak from a background. Our experience shows that it is useless to look for an universal peak-background threshold common for all events of a given experimental run, since this threshold strongly depends on the informative load of the given event. Aiming for statistical efficiency of our method we elaborated the following heuristic formula for the peak-background threshold of a particular event:

$$N_{\text{bound}} = C * H_{\text{max}} + H_{\text{mean}}, \quad (5)$$

where  $H_{\text{max}}$  is the maximum value of the histogram,  $H_{\text{mean}}$  is its mean value,  $C$  is a constant, which value is to be tuned to the given experiment data.

Choosing the bin size, one should find a reasonable compromise between either a too small or too big bin size. The first case could lead to the histogram peak loss, i.e. to losing one of the tracks, while a too big bin size decreases the accuracy.

#### 4. Robust fitting

The direct application of the conventional least square method (LSM) for our problem conflicts with the fundamental LSM assumptions. Firstly, the deviations (3) in LSM function (1) are not normally distributed. Furthermore, we do not fit a circle to a set of measured points, as in the conventional LSM, but again our circular track is to be fitted to the SC set  $S = \{x_i, y_i; r_i, i = \overline{1, N}\}$ . In addition, the influence of point-outliers on parameter estimations is excessive due to squaring of each deviation’s value in the LSM function (1). This makes the whole problem ill-posed.

However, the above-mentioned concept of the tangency measure for two circles allows us, as in the previous section, to replace each SC by two points of the possible SC-tangency with the track. Those two points can be calculated as the crossing points of SC with the straight line between the SC-center and the center of the circle arc serving as the track model. As stated above, the set  $S$  includes triplets  $(x_i, y_i; r_i)$  produced by one of tracks and also by some noise tubes. Thus we have a kind of a contaminated sample and, therefore, can use the *robust* approach invented

in [9] by analogy to P. Huber's M-estimates [21]. Due to the LSM violations, the maximum likelihood approach should be applied. It was done in [9] under the assumption that the contaminating points are uniformly distributed. By differentiating the logarithmic likelihood function for measured point deviations (3), the search of its maximum was reduced to the iterative solution of a normal equation system for unknown parameters with the special optimal weights recalculated on each iteration step as functions of those deviations.

This approach was then applied to the circle fitting problem in [16,15], where the optimal weights were approximated by the 4th order polynomial that, in fact, coincides with Tukey's famous bi-square formula [22],

$$w_i^k = \begin{cases} (1 - ((d_i^{(k-1)}) / (c_T * \hat{\sigma}^{(k-1)}))^2)^2 & \text{if } |d_i^{(k-1)}| \leq c_T * \hat{\sigma}^{(k-1)}, \\ 0 & \text{otherwise,} \end{cases} \quad (6)$$

where  $k$  is the iteration number,  $d_i^{k-1}$  is the residual of the deviations obtained at the previous iteration, and  $\hat{\sigma}^{(k)}$  is the estimate of variance evaluated as

$$(\hat{\sigma}^{(k)})^2 = \sum w_i^{(k)} (d_i^{(k)})^2 / \sum w_i^{(k)}.$$

Since the SHPM-procedure provides us with initial values of parameters, we use them to calculate  $w_i^0$ . The constant  $c_T$  is an external parameter of the robust fitting algorithm. The latter was taken from [13] with the robust modifications described in detail in [16]. For our calculations we vary the constant  $c_T$  and obtain the best results for  $c_T \simeq 3$ .

## 5. Elastic arm (deformable template) approach

Elastic arm methods, known also as deformable template methods (DTM), represent an effective association between neuron decision and parameter fitting. In other neural network or classical pattern recognition approaches, one has then to provide the algorithm with some fitting procedure. So it is advantageous to have an algorithm that does both the assigning and the fitting simultaneously. The elastic arms strategy is to match templates, i.e. simple parameterized models (which in our case are circle arcs) to observed objects (small circles from  $S$ ). An unknown subset

of these objects corresponds to noise and should be unmatched.

Having objects different from just measured points as it was in known DTM applications [10,11], we have to modify the definition of the binary decision unit (neuron). Similar to [17,18] we define it as a two-dimensional vector  $s_i = (s_i^+, s_i^-)$  with admissible values (1,0), (0,1), (0,0). Denoting the measurement error of the drift radius by  $\lambda$  we introduce the energy function of our neural system as the following functional  $L$ :

$$L(a, b, R, s_i^-, s_i^+) = \sum_{i=1}^N \{d_i^- s_i^- + d_i^+ s_i^+ + \lambda((s_i^- + s_i^+) - 1)^2\}. \quad (7)$$

Circle parameters ( $a, b, R$ ) that correspond to a track in question would define a point in the parameter space, where this functional  $L$  has to reach its global minimum. Since each SC can belong only to one of the tracks or to no track at all,  $L$  must be minimized with the following conditions:  $s_i = (0,0)$  means  $i$ th tube for the given track is the noise tube and the combination  $s_i = (1,1)$  is forbidden, i.e.

$$s_i^+ + s_i^- \leq 1. \quad (8)$$

The initial values of the track parameters can be obtained from the previous stage of robust fitting (or if you want to apply DTM directly, by the SHPM). Then choosing an area where this track could lie, we proceed to look for a global minimum of the functional  $L(a, b, R, s_i^-, s_i^+)$  (7). One of the main problems here is how to avoid local minima of  $L(a, b, R, s_i^-, s_i^+)$  provoked by the stepwise character of the vector  $s_i = (s_i^+, s_i^-)$  behavior. One of the known ways to avoid such an obstacle is the standard mean field theory (MFT) approach leading to the simulated annealing method [23]. Our system is considered as a thermostat with the current temperature  $T$  [10]. Then as it was shown in [17], parameters  $s_i^+, s_i^-$  of the functional  $L(a, b, R, s_i^-, s_i^+)$  with fixed ( $a, b, R$ ) can be calculated by the following formulae, where the vector  $s_i$  with its stepwise behavior is replaced, in fact, onto sigmoidal Potts factors:

$$s_i^- = \frac{1}{1 + e^{(d_i^- - \lambda)/T} + e^{(d_i^- - d_i^+)/T}}, \quad (9)$$

$$s_i^{\pm} = \frac{1}{1 + e^{(d_i^+ - \lambda)/T} + e^{(d_i^+ - d_i^-)/T}} \quad (10)$$

There are many parameters that must be properly set up, since neural networks are very sensitive to them. One of them is the temperature. So we try to keep a balance between the total DTM speed and the needed number of temperature steps in the simulated annealing scheme. Thus the  $L$  global minimum is calculated according to the following:

- (1) Three temperature values are taken: high, middle and a temperature in the vicinity of zero, as well as three noise levels corresponding to them [17,10].
- (2) According to the simulated annealing scheme, we start from high temperature. With initial circle values  $(a_0, b_0; R_0)$  parameters  $s_i^+, s_i^-$  are calculated by formulae (9), (10).
- (3) For the  $(s_i^+, s_i^-)$  obtained, new circle parameters  $(a, b; R)$  are calculated by modification of the standard gradient descent method. This modification consists of the individual updating of the  $L$  parameters and holding a condition

$$L(a_k, b_k, R_k) < L(a_{k+1}, b_{k+1}, R_{k+1}) \quad (11)$$

- (4) The stopping rule is as follows: either

$$|L(a_k, b_k, R_k) - L(a_{k+1}, b_{k+1}, R_{k+1})| < \epsilon \quad (12)$$

holds or the iteration number exceeds a prescribed number  $k = \text{const}$ .

- (5) If the conditions of step (4) are not satisfied, then with the new circle parameters  $(a_{k+1}, b_{k+1}, R_{k+1})$ , the next values of  $s_i^+, s_i^-$  are again calculated by (9), (10), and we go to step (3).
- (6) After the process converges, the temperature is changed (the system is cooled). The values of  $(a, b, R)$  attained with the previous temperature are taken as starting values, and we go to step (2) again.
- (7) With each temperature value, after completing step (5) the condition

$$L < L_{\text{cut}} \quad (13)$$

is tested. If it fits, our scheme is completed and the algorithm proceeds the next stage of correcting the obtained track parameters  $(a, b, R)$ .

Otherwise, if at a temperature in the vicinity of zero we obtain

$$L > L_{\text{cut}}, \quad (14)$$

the track finding scheme failed.

## 6. Procedure of the track parameter correction

The robust and deformable template methods provide us with the track parameters  $(a, b; R)$ . However, these parameters, even if they satisfy (13), could be far from the global minimum of  $L$ . Therefore, we have to elaborate an extra step for a possible track parameter correction. The idea is to improve the procedure described in Section 3 for converting the measured data from the set  $M$  format to the  $\Omega$  set. Determination of two points on each small circle of the set  $M$  was done too roughly and produced a left-and-right (or top-and-down) uncertainty. Now having the track-candidate parameters  $(a, b; R)$  and the concrete values of vectors  $s_i = (s_i^+, s_i^-)$ , or  $w_i$ , we can make this procedure more accurate. On each SC of the set  $S = \{x_i, y_i; r_i, i = \overline{1, N}\}$  the point can now be found that is nearest to the track-candidate with respect to values of  $s_i$  or  $w_i$ . Then all these found points are approximated by a circle, and the  $\chi^2$  value is calculated as the goodness-of-fit criterion.

If  $\chi^2 < \chi_{\text{cut}}^2$ , the approximating parameters  $(a, b; R)$  are accepted as the likeliest. Otherwise, the track-candidate is rejected.

## 7. Results and concluding remarks

The proposed track-finding algorithm of the tracks detected by the MDT system in a magnetic field was tested on different series of simulated events. The MDT model, as it shown in Fig. 1, consists of 6 superlayers formed by three single layers arranged in honeycomb order. The distance between the first layer and the last one is 1040 mm. Events were generated for the most extreme situation, when two circular tracks always crossed each other under the narrow angle and noise signal is produced by one of ten tubes in each layer. The radii of simulated tracks were kept in the range of 1–3 m with the same sign of the curvature.

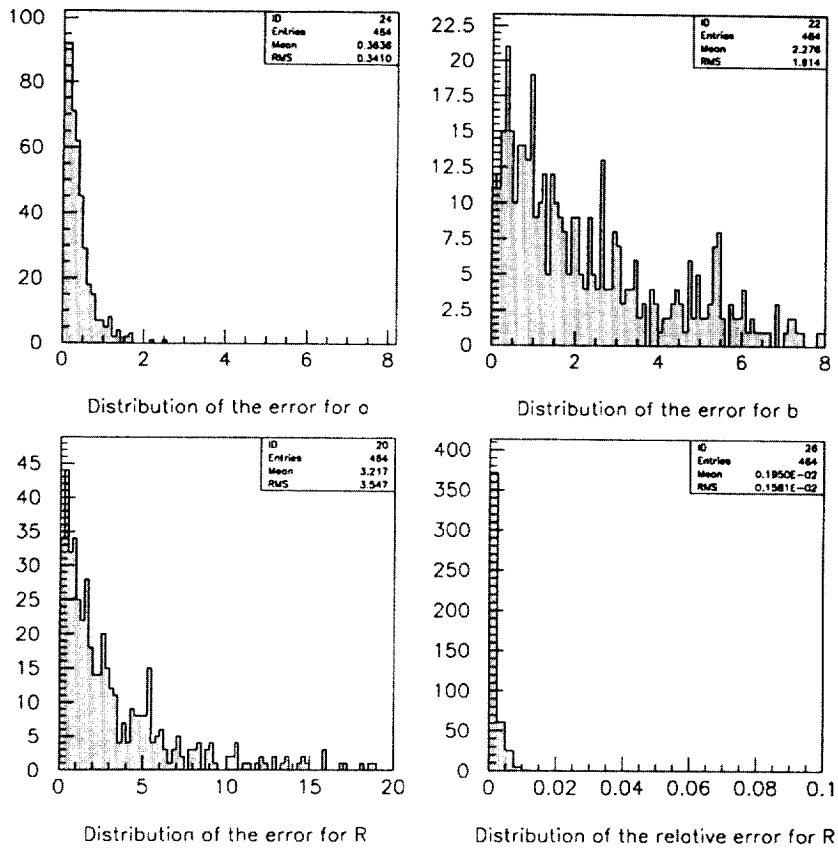


Fig. 2. Distribution of the error of the circle parameters for deformable templates only. Measurement error  $\lambda = 0.2$  mm.

On Fig. 1 you can see the typical example of the tested events.

The sample of different groups of  $\sim 500$  simulated events was tested by two track finding algorithms:

- (i) deformable template method (DTM) only;
- (ii) the hybrid method combined both: robust and deformable template methods

Even in such heavy conditions the efficiency of the correctly recognized events is in the range of 94–96% for the first (DTM) algorithm. For the second hybrid algorithm it is slightly higher: 96–98% (for the well separated tracks it goes up to 99%).

Figs. 2 and 3 show the error distributions for the circle parameters ( $a$ ,  $b$ ,  $R$ ) for the first and the second algorithms correspondingly, i.e.

$$|a_{\text{find}} - a_{\text{model}}|, \quad |b_{\text{find}} - b_{\text{model}}|, \\ |R_{\text{find}} - R_{\text{model}}|, \quad \frac{|R_{\text{find}} - R_{\text{model}}|}{R_{\text{model}}}.$$

The accuracy of  $R$ , which is proportional to the particle momentum, looks quite good. The notable difference in accuracy of  $a$  and  $b$  was expected due to the relatively small angle size of the measured circle arc.

Thus, comparing results of both algorithms we conclude that, although the hybrid method is slightly less accurate than DTM (less than 1%), its faster robust stage<sup>3</sup> gives satisfactory results in  $\sim 90\%$  of all events, when the process is finished. So we gain in speed with a prescribed level of accuracy.

It should be pointed out that the main time waster of the whole program is the SHPM realization of the Hough transform. Due to the effect of point doubling for each SCs, the initial stage of SHPM search wastes more than 95% of the total calculation time. It is clear that for the mass processing of future real ATLAS data it will be needed either to use the RPC data for

<sup>3</sup> See [13] where the robust algorithm timing is indicated.

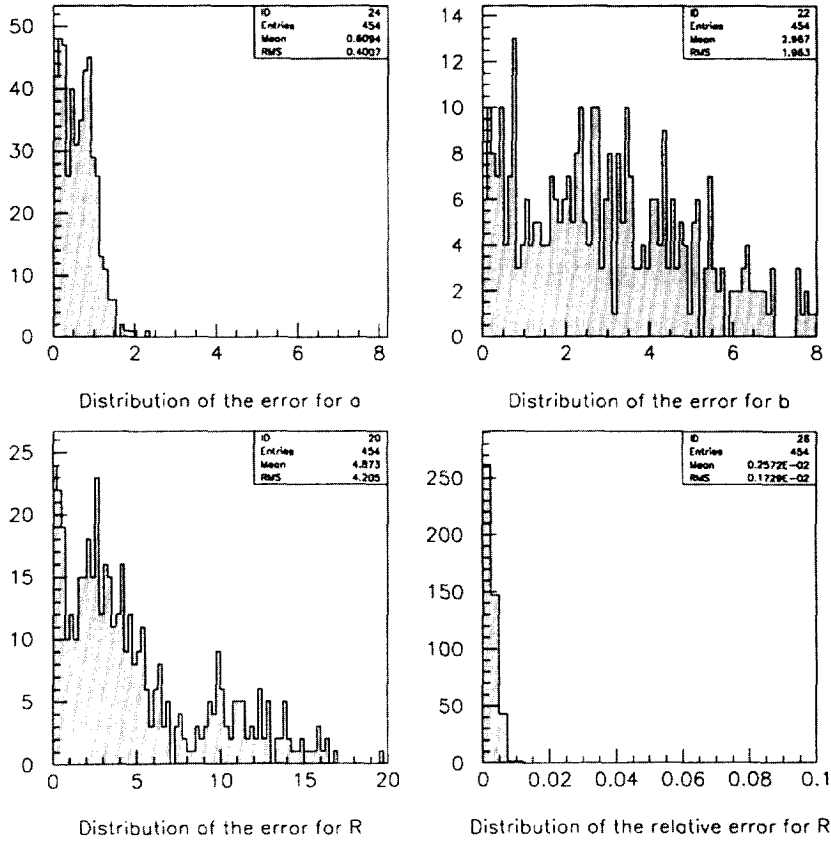


Fig. 3. Distribution of the error of the circle parameters for the hybrid method. Measurement error  $\lambda = 0.2$  mm.

providing the initial parameter values or to implement the SHPM algorithm by hardware.

Fig. 4 shows the result of exploring how the radius of the found tracks depends on the measurement error of the drift radius. For the different values of the measurement error a mean value of the error  $|R_{\text{find}} - R_{\text{model}}|$  was estimated. This is shown by a continuous line in Fig. 4. The dotted line shows the maximum value  $|R_{\text{find}} - R_{\text{model}}|$  for the same events. The range of the measurement error was, in fact, prolonged to 1 mm, but since it leads to a sharp decrease of the recognition efficiency (below 90%) those results are not included in Fig. 4.

In conclusion, we can say that the proposed hybrid algorithm achieved its main aims in the processing of MDT simulated events in accuracy, efficiency and speed. The obtained results are accepted as quite satisfactory for the present stages of both experiment ATLAS and EVA/E850 [18,24,25].

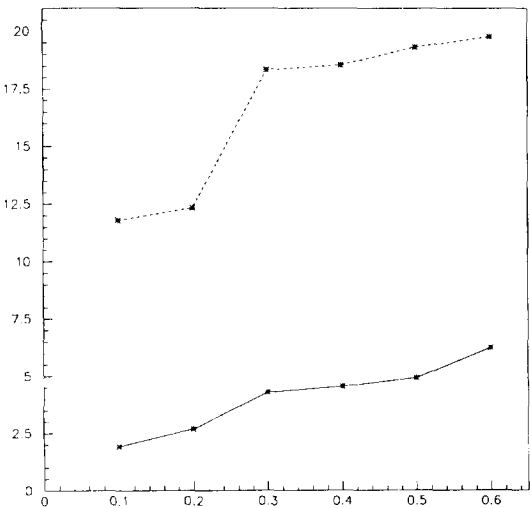


Fig. 4. Dependence of the drift radius error of the recognized tracks upon the measurement error. X, Y-axes in mm.



## Acknowledgements

The authors express their gratitude to professor G. Chelkov for simulating this work and the doctors R. Airapetyan and I. Alexandrov for fruitful discussion and valuable advice.

## References

- [1] H. Grote, Pattern recognition in High Energy Physics, CERN 81-03 (1981).
- [2] G. Ososkov, Applications of pattern recognition methods in high energy physics, JINR Commun. 10-83-187, Dubna (1983) [in Russian].
- [3] Frühwirth, Nucl. Instr. & Meth. A 262 (1987) 444.
- [4] C. Peterson, B. Söderberg, Int. J. Neural Syst. 1 (1989) 3.
- [5] S. Baginyan, A. Glazov, I. Kisel, E. Konotopskaya, V. Neskromnyi, G. Ososkov, Tracking by modified rotor model of neural network. Comput. Phys. Commun. 79 (1994) 165–178.
- [6] ATLAS Technical Proposals, CERN/LHCC/94-43, LHCC/P2, 15 Dec 1994.
- [7] J. Wu, E.D. Minor, J.E. Passaneau et al., The EVA trigger: Transverse momentum selection in a solenoid, Nucl. Instr. & Meth. Phys. Res. A 349 (1994) 183–196.
- [8] R. Mankel, Pattern recognition algorithm for B meson reconstruction in hadronic collision, in: Proc. of CHEP'97, Berlin, April 7–11, 1997, DESY (1997) pp. 23–27.
- [9] G. Ososkov, Robust regression for the heavy contaminated sample, Proc. 2d Tampere Conf. in Statistics, Univ. of Tampere (1987) pp. 615–626.
- [10] M. Ohlsson, C. Peterson, A.L. Yuille, Track finding with deformable templates – the elastic arm approach, Comput. Phys. Commun. 71 (1992) 77.
- [11] L. Muresan, R. Muresan, G. Ososkov, Yu. Panebratsev, Deformable templates for circle recognition, JINR Rapid Commun. I[81]-97, Dubna (1997).
- [12] J.F. Crawford, Nucl. Instr. & Meth. 211 (1983) 223.
- [13] N.I. Chernov, G.A. Ososkov, Effective algorithm for circle fitting, Comput. Phys. Commun. 33 (1984) 329–333.
- [14] V. Karimäki, Effective circle fitting for particle trajectories, Nucl. Instr. & Meth. A 305 (1991) 187–191.
- [15] G. Agakichiev, A. Drees, P. Glässel, D. Irmscher, G.A. Ososkov, Y. Panebratsev, A. Pfeiffer, H.J. Specht, V. Steiner, I. Tseruya, T. Ullrich, Cherenkov ring fitting techniques for the CERES RICH detectors, Nucl. Instr. & Methods A 371 (1996) 243–247.
- [16] N.I. Chernov, G.A. Ososkov, Fast programs for circle fitting, in: Collect. Sci. Papers, Vol. 5, KFKI-1987-17/M, KFKI, Budapest (1987) pp. 51–64.
- [17] S. Baginyan, S. Baranov, A. Glazov, G. Ososkov, Application of deformable templates for recognizing tracks detected with high pressure drift tubes, JINR Commun. E10-94-328, Dubna (1994).
- [18] S. Baginyan, S. Baranov, A. Glazov, G. Ososkov, Application deformable templates method the recognition of tracks, detected by High Pressure Drift Tubes, ATLAS Internal Note, MUON-NO-51, CERN (1994).
- [19] R.O. Duda, P.E. Hart, Pattern Classification and Scene Analysis (Wiley, New York, 1973).
- [20] Yu.A. Yatsunenko, Nucl. Instr. & Meth. A 287 (1990) 422–430.
- [21] P. Huber, Robust Statistics (Wiley, New York, 1981).
- [22] F. Mosteller, W. Tukey, Data analysis and regression: a second course in statistics (Addison-Wesley, Reading, MA, 1977).
- [23] S. Kirkpatrick, C.D. Gelatt, M.P. Vecchi, Optimization by simulated annealing, Science 22 (1983) 671.
- [24] S. Baginyan, An algorithm for recognition of curve tracks detected by drift tubes of the muon spectrometer, JINR Commun. E10-96-366, Dubna (1996).
- [25] S. Baginyan, G. Ososkov, Yu. Panebratsev, S. Shimanskiy, Algorithm for recognizing tracks detected by drift tubes in a magnetic field, JINR Commun. E10-96-263, Dubna (1996).